

NPS67-83-004CR

NAVAL POSTGRADUATE SCHOOL

Monterey, California



CONTRACTOR REPORT

A Review of the Design of the NPS/TPL
Transonic Compressor

J. R. Erwin

March 1983

Contractor Report

Approved for public release; distribution unlimited

Prepared for:

Naval Postgraduate School
Monterey, California 93943

FedDocs
D 208.14/2
NPS-67-83-004CR

NAVAL POSTGRADUATE SCHOOL
Monterey, California

Commodore R. H. Shumaker
Superintendent

D. A. Schradly
Provost

The design review reported herein was carried out for the Naval Postgraduate School by the author under Work Order N0001981WR11104, under Contract Number N62 271-81-M-1436. The work was associated with the program entitled Transonic Compressor Investigations funded in part under the Air Breathing Propulsion Research Program by Naval Air Systems Command, Code Air 310E.

This report was prepared by:

(Deceased)

J. R. ERWIN

Publication of the report does not constitute approval of the sponsor for the findings or conclusions. It is published for information and for the exchange and stimulation of ideas.

REPORT DOCUMENTATION PAGE		READ INSTRUCTIONS BEFORE COMPLETING FORM
1. REPORT NUMBER NPS-67-83-004CR	2. GOVT ACCESSION NO.	3. RECIPIENT'S CATALOG NUMBER
4. TITLE (and Subtitle) A Review of the Design of the NPS/TPL Transonic Compressor		5. TYPE OF REPORT & PERIOD COVERED Contractor Report (Project) June 1981-August 1981
		6. PERFORMING ORG. REPORT NUMBER
7. AUTHOR(s) J. R. Erwin		8. CONTRACT OR GRANT NUMBER(s) N62 271-81-M-1436
9. PERFORMING ORGANIZATION NAME AND ADDRESS Naval Postgraduate School Monterey, California 93943		10. PROGRAM ELEMENT, PROJECT, TASK AREA & WORK UNIT NUMBERS 61153N, RR024-03-01 N0001981WR11104
11. CONTROLLING OFFICE NAME AND ADDRESS Naval Air Systems Command Washington, DC 20361		12. REPORT DATE March 1983
		13. NUMBER OF PAGES 41
14. MONITORING AGENCY NAME & ADDRESS (if different from Controlling Office) Naval Postgraduate School Monterey, CA 93943		15. SECURITY CLASS. (of this report) UNCLASSIFIED
		15a. DECLASSIFICATION/ DOWNGRADING SCHEDULE
16. DISTRIBUTION STATEMENT (of this Report)		
17. DISTRIBUTION STATEMENT (of the abstract entered in Block 20, if different from Report)		
18. SUPPLEMENTARY NOTES		
19. KEY WORDS (Continue on reverse side if necessary and identify by block number) Axial Compressor Transonic Compressor Compressor Design		
20. ABSTRACT (Continue on reverse side if necessary and identify by block number) The design of a small transonic research compressor is reviewed briefly. The design was one carried out by M. H. Vavra before 1970 without resort to computer programs. The effect of an error made in the calculation of setting angles for the rotor blading is judged to be serious near the blade tip. A possible mismatch to the stator is suggested and it is recommended that the possibility of structurally correcting the stagger at the tip be considered.		

COMMENT

A review of the design of the NAS/TPL compressor was requested because no formal report on the design had been written by the designer, Dr. M. H. Vavra, at the time of his death in May 1975. An error had been found subsequently by the undersigned in design calculations contained in design note books. The error (discussed at length in the present report) led to a mis-setting of the blades on the rotor, and a consequent mismatch to the stator blade row. The present design review was requested because, in spite of the design error, the efficiencies obtained in tests to 70% design speed were surprisingly high (87%).

It is noted that the present report was not fully typed at the time of the author's death in May 1983. It is issued now for the information which it contains and for the purposes of record. The report does not explain the high efficiencies observed in tests, nor does it attempt to analyze the degree of rotor-stator mismatch. Also, no comment is made on the design assumption of uniform axial velocity into the rotor, which would not be the case with the designed inlet geometry. It was not possible apparently for the author to reconstruct the radial equilibrium calculations from the designer's notes, and an independent analysis was not attempted.

The present stage has served well to develop testing and advanced instrumentation techniques. An experimental and analytical study of the internal aerodynamics of the stage has been made and will soon be reported.

R. P. SHREEVE
Director
Turbopropulsion Laboratory

TABLE OF CONTENTS

<u>Section</u>	<u>Page</u>
1. INTRODUCTION	1
1.1 History of Project and Dr. Vavra's Role	1
1.2 Purpose of the Program	2
1.3 Background Considerations	2
1.4 How It Was Done	3
1.5 Error and Its Influence	4
1.6 Guide to Report	5
2. DESIGN OF THE TRANSONIC STAGE	7
2.1 Design Requirements and Approach	7
2.2 Velocity Diagrams and Flow Parameters	9
2.3 Blade and Vane Selection	9
2.4 Structural Considerations	11
3. INDUCTION SYSTEM	12
4. DIFFUSER	15
5. INSTRUMENTATION	16
6. CONCLUDING REMARKS	18
APPENDIX A. Exploratory Studies for the Design	28
APPENDIX B. Rotor Blade Vibration Measurements	30
APPENDIX C. Symbols	38

LIST OF ILLUSTRATIONS

	<u>Page</u>
1. Rotor Blade Setting Angle	21
2. Design Campbell Diagram for the Transonic Rotor . . .	22
3. Transonic Compressor Test Rig (not to scale)	23
4. Transonic Compressor (TPL DWG 2147-2)	25
5. Structural Detail of the Test Compressor	27
B1. Transonic Compressor	35
B2. Frequency-Speed Diagram for Blade Vibrations From Shaker-Table Tests of the Transonic Compressor Rotor	37

I. INTRODUCTION

1.1 History of Project and Dr. Vavra's Role

The Naval Postgraduate School (NPS) transonic axial compressor aerodynamic and mechanical design was conducted by Dr. M. H. Vavra between April 17 and July 17, 1968. All the calculations were done by Dr. Vavra by hand and slide rule. All drawings of the compressor and of the complete test rig (including the twin-turbine drive) were done by Dr. Vavra. The contrast of this individual effort with today's industrial design system wherein separate teams do aerodynamic, mechanical, instrumentation and test facility design, often by use of programs buried deep in a main-frame computer, is striking. Over-specialization may have set in; at least a partial return to the generalist seems in order to permit new generations of engineers to develop a feeling and respect for the physical flows and forces that exist, how the design systems came about, and what their limitations are. Individual efforts can be carried too far, however. In this transonic compressor design, a simple error in sign occurred when the setting angle relation was transferred to a calculation table. With no one checking the numbers, the error was built into the rotor blades, so that the intended design was not achieved.

1.2 Purpose of the Program

The purposes of the NPS transonic compressor program were several:

- To design and develop an advanced test vehicle useful in providing "hands-on" operating experience for naval officers in fields of aerodynamic, mechanical and electronic engineering.
- To develop simplified aerodynamic design methods for teaching purposes.
- To demonstrate a transonic compressor having potential use in military propulsion systems.
- To provide a test vehicle in which detailed measurements of flow structure within rotor and stator blading could be made. Improved methods for axial flow compressor design and analysis were the overall goal.

1.3 Background Considerations

The very good performance of the General Electric Transonic Rotor 1B (NASA CR 54581 and 54582) was known at the time the NPS transonic compressor design began. Rotor 1B was designed for a tip rotational speed of 1400 fps and with a tip diffusion factor of 0.35. Under uniform entrance conditions this rotor exceeded its design total pressure ratio, 1.6, airflow, 215 lbs/sec and efficiency, 85.7%, by very satisfactory margins. The tip Mach number of rotor 1B was 1.40, with a rotor inlet hub-to-tip radius ratio of 0.50. Rotor 1B used circular arc sections for the inner 60% of the blade span and multiple-circular-arc sections having rearward loading in the outer 40% span. At 105% speed, or $U_{tip} = 1470$ fp, Rotor 1B showed 88% rotor adiabatic

efficiency maximum and maintained a similar rotor efficiency when performance with 15% stall margin was measured at this same speed. The potential performance of a transonic axial compressor stage designed and matched for a tip rotational speed in this range looked very good.

1.4 How It Was Done

The aerodynamic flow through this compressor was calculated as a series of successive approximations using potential flow methods described in Chapter 16 of Reference 1. The first approximation employed constant axial velocity using the value found at the tip section (selected as a constant radius from rotor leading edge to stator trailing edge). Total pressure ratio equal to that estimated at the tip was selected at all radii, with an appropriate efficiency estimated to occur at each radius. An iteration involving flow density, continuity, and exit tangential velocity ensued which yielded the exit radius for each of 5 streamlines bounding 4 axisymmetric streamtubes of equal mass flow.

From the first approximation streamline slopes and curvatures upstream and downstream of the rotor could be obtained for use in solving the equations defining the variation of meridional velocity with radius.

From the results of these solutions an approximation was made using the same method. The changes in meridional velocity between second and third approximation were small.

1.5 Error and Its Influence

When the setting angle, λ , of the rotor blade sections was being calculated, an error in sign of the relation between angle and camber incidence and deviation angles was made when the equation was transferred to the calculation sheet. This typographical error was not detected until after the blades were machined. The design setting angle and the actual setting angle are presented in Figure 1.

The setting error is serious only in the outer 25% of the passage area. In the inner 75% of the flow path area, the error is either relatively small or, in the root region, may have inadvertently set the sections open an amount which will compensate for an underestimation of the deviation angle which will occur. Recent experience with transonic rotors of this type have shown significantly more deviation in the hub region than the correlations of NASA SP-36 indicate (see NASA CR121095). The incidence change from about -1.5° to about $+1.5^\circ$ at the root section is not likely to be detrimental since the throat area will be increased and the throat Mach number reduced by this change to a more open hub setting.

The blade setting error in the outer 25% of the flow path area is serious, particularly at the tip section. The design intent was to operate this section at an incidence of -2.8° with an air turning angle of $+0.58^\circ$. The rotor tip setting is actually 5.6° more open. The first order effects of this increased incidence are to increase the tip loading significantly and to increase the supersonic expansion of the flow

around the leading edge. Although the effects will be alleviated somewhat by an increased axial velocity in the tip region due to the lower static pressure produced by the increased supersonic expansion, the net effect will be a stronger shock system at the tip with increased flow separation from the rotor blade suction surface and from the adjacent casing. Increased losses in the tip region will surely result.

If these expectations are borne out by high speed test results, the possibility of twisting the rotor blade tips closed by 5.6° should be considered. Specimens of a similar shape, of the same aluminum alloy and heat treatment should be twisted to determine whether the metal can withstand local twisting of this amount. This practice is common during the development of axial compressors for aircraft gas turbines, but frequently the result is less uniformity than is desirable in a research compressor stage. With sufficient care, an acceptable job of twisting the rotor blade tips can probably be achieved if the metal will not be weakened significantly.

1.6 Guide to Report

This paper is primarily intended to present the details of the NPS transonic compressor design (which was done by Dr. M. H. Vavra in 1968) for the record. The introduction presents the history and purpose of the project, the logic of the design, and notes an error in sign made in setting the rotor blade sections. A brief discussion of the effect of this error on the expected performance and a suggestion concerning a corrective twist to each rotor blade are presented.

The aerodynamic and mechanical designs are presented in Section 2, followed by sections describing the air inlet system, the exit diffuser, and provisions for instrumentation. Concluding remarks and recommendations for future investigations end the main body of this report. Appendices follow which present the symbols used and describe exploratory studies which were conducted and rotor vibration measurements.

2. DESIGN OF THE TRANSONIC STAGE

2.1 Design Requirements and Approach

This transonic compressor was intended to produce a high stage pressure ratio at high efficiency while pumping at a relatively high specific flow capacity. In order to accomplish these objectives, a tip Mach number of $M = 1.50$ was selected as the highest value for which acceptable rotor performance had been demonstrated up to 1968, the time the design was begun. An inlet flow angle relative to the rotor tip of $\beta = 65^\circ$ was selected somewhat arbitrarily, but the choice resulted in a tip rotational speed of 1462 fps and a moderately high axial flow Mach number ($M_a = .634$) which met the performance requirements for the compressor very satisfactorily. This tip rotational speed in conjunction with the selected rotor inlet hub-to-tip radius ratio, $R_H/R_T = 0.50$, would not overstress high strength aluminum alloys which are easily machined. The value of axial Mach number provides a flow capacity within 13% of the maximum possible per unit annulus area. This annulus flow rate and the flow area available with the R_H/R_T selection yield a satisfactorily high flow capacity.

The rotor inlet hub-to-tip radius ratio of 0.5 was probably selected on a compromise basis between this value and a lower one which would have yielded a slightly higher mass flow per unit frontal area (specific flow capacity) but which would have made machining the integral rotor blades

more difficult, more time-consuming and more expensive. The choice of constant axial velocity upstream and downstream of the rotor and stator was made as a first approximation.

The rotor tip D factor was selected as the maximum value observed near rotor tips before excessive losses occur (NASA SP-36). This design approach was a little unusual since in most industrial applications a particular pressure ratio is required to meet gas turbine cycle thermodynamic requirements or to produce a desired fan thrust. This approach probably yields the appropriate total pressure ratio for maximum efficiency at the Mach number (1.5) selected for this rotor. Conceivably, the same total pressure ratio could be produced with a slightly higher efficiency using a lower rotational speed. Such an optimization study has not been conducted, however. The work input resulting from the selected values at the tip (constant radius) is

$$\dot{m} C_p \Delta T_t = \dot{m} U \Delta V_\theta = 1462 \times 437.3 M = 639,332.6 \text{ ft-lb/slug}$$

or

$$\Delta T_t = 639,332.6 / 6006 = 106.4^\circ.$$

Using a nominal efficiency, $\eta = 80\%$ (prior to loss estimations and efficiency calculations) the stage total pressure is

$$P_{T_3} / P_{T_1} = \left[\frac{T_{T_0} + \eta \Delta T_t}{T_{T_0}} \right]^{\frac{\gamma}{\gamma-1}} = \left[\frac{520 + (0.80)(106.4)}{520} \right]^{3.5}$$

$$= (1.1637)^{3.5} = 1.70$$

Note by reviewer: Similar calculations for mean line and hub streamlines give ΔT 's of $80.5^\circ R$ and $75.9^\circ R$ respectively. An attempt appears to have been made to design for uniform total pressure rise through the rotor to give a stage pressure ratio of 1.5 to 1.6.

A transonic compressor stage having a total pressure of 1.70, a high specific flow and an efficiency of 80 to 90% would be a useful contribution, with the value increasing as the efficiency increases, for application as a separate fan or as a stage in a multistage axial-flow compressor. This was particularly true in 1968 at the time the design was conducted, but it is still true more than a decade later.

Design data for the air turbine used to drive the compressor (powered by an Allis-Chalmers continuous air supply) are given in Table I. Design point data for the compressor are listed in Table II.

2.2 Velocity Diagrams and Flow Parameters

Velocity diagram data resulting from a hand-iterated streamline curvature solution for the axisymmetric through-flow at design conditions, are listed in Table III.

2.3 Blade and Vane Selection

The rotor blade and stator vane designs were selected using NASA methods described in NASA SP-36 (Ref 2) and in extensions of these methods described in Appendix B of NASA TN D-3959 (Ref 3). Arbitrary section solidities and thicknesses were initially selected. The rotor and stator solidities were optimized aerodynamically as described below. Section thicknesses near the rotor hub were finally selected on the basis of stress and vibration calculations conducted after the aerodynamic design was essentially complete.

Because of the high Mach number relative to the rotor tip, $M = 1.5$, a thin circular arc section was selected for

this radius. Although NACA 65 Series Airfoil sections would have been satisfactory at the hub and inner radii, ease of specification and machining led to the use of circular arc sections for all rotor streamlines. Circular arc sections were selected for all stator streamlines probably because the maximum entering Mach number was 0.91, rather high for 65-series sections.

Using the loss correlation methods presented in Reference 2 (NASA SP-36), values of the loss coefficient, $\bar{\omega}$, are found as a function of the diffusion factor, D ; where

$$\bar{\omega} = \frac{P_{T1} - P_{T2}}{P_{T1} - P_1}$$

$$D = 1 - \frac{V_2}{V_1} + \frac{R_2 V_{\theta 1} - R_1 V_{\theta 1}}{(R_1 + R_2) \sigma V_1}$$

for a range of solidities, $\sigma = c/s$, for each streamline vector diagram of the rotor or stator. Knowing the appropriate exit flow direction, β_2 , from the rotor (or α_2 from the stator) the total pressure loss coefficient, $\bar{\omega}$, may be estimated from the following relation:

$$\bar{\omega} = \frac{2\sigma\Omega}{\cos \beta_2} .$$

The values of total pressure loss parameter Ω were obtained from the appropriate curve given in Figure 5 of Reference 3 (NASA TND 3595).

For flow angles, $\beta_{2R} > 45^\circ$, the correlation

$$\bar{\omega} = 2\sqrt{2} \sigma_R \Omega_R \left[1 - \frac{\pi}{4} + \frac{\pi}{180} \cos \beta_2 \right]$$

from Ref 3 (NASA TND 3595) was used.

The initial selection of the double-circular arc rotor blade sections led to a rotor blade pressure surface composed of concave sections inboard with flat or convex sections outboard. The change of sign in surface curvature complicated and made more expensive the machining of the internal bladed rotor. Trade-offs between incidence and camber were made to yield all rotor blade sections with straight pressure surfaces.

2.4 Structural Considerations

The maximum steady state tension stress in the aluminum alloy (Al 7178-TG) blades was calculated to be 27,300 psi at the blade root. The bending stress due to aerodynamic loading was calculated to be 8180 psi for 500 hp absorption at 30,460 rpm, the design speed. These stresses, when added, are well below the 0.2% elongation strength of 78,000 psi for this alloy, but well above the long-time fatigue strength of 22,000 psi given for this material. A generous fillet having a maximum width equal to 24% of the maximum section thickness was added at the root to bring the stresses within the long-time fatigue limit. Using the relation that the maximum oscillatory stress is 40% of the product of steady state bending stress, and the stress concentration factor, 1.2, a figure of about 4,000 psi additional stress due to vibration was estimated.

3. INDUCTION SYSTEM

The compressor air flow enters the test system from the atmosphere through gauze filters contained in one end of a small wood shelter (Fig. 3). The shelter also houses the intake throttle valve which consists of two closely-spaced plates having the same hole pattern. Throttling is accomplished by rotating one plate with respect to the other. The throttle is followed by a 32" diameter settling chamber equipped with a perforated plate and four screens. A bell-mouth leads into an 18" diameter pipe which contains a standard long-radius measuring nozzle. A straight run of 18" pipe about 7.5 diameters long precedes the final contraction just upstream of the 11" diameter test compressor. Compressor air flow rate is calculated from the measured inlet total pressure and total temperature and the pressure difference between the inlet total pressure and the nozzle throat static pressure.

Figure 4 shows a break in the flow path between the flow nozzle and the compressor outer casing. The flow nozzle was moved upstream and the discontinuity was eliminated through use of a fairing. After passing through the test compressor, the flow is returned to the axial direction in a high solidity honeycomb, through a diffuser which turns the flow to the radial direction and discharges to the atmosphere.

If the blades are not operated in a vibratory mode for more than a few seconds, the blade strength appears to have adequate safety factor for research purposes.

The bending frequencies were calculated to be 51,840, 323,500 and 908,600 rpm or 864, 5,392 and 15,143 hertz for the first, second and third modes, respectively, ignoring the stiffening effect due to rotation. Torsional vibrational frequencies of 274,060, 822,100 and 1,370,000 vpm or 4,568, 13,702, and 22,833 hertz were calculated for the first, second and third modes, respectively.

A Campbell Diagram plotting cycles per minute versus rotor revolutions per minute and showing lines of intersections per minute for intersections which occur once per revolution, twice per revolution, etc., was prepared. The intersections of first and second bending frequencies and first torsional frequency with various potential distortion rates (once per rev, etc.) were shown (Fig 2). Twenty-three stator vanes might excite the second bending mode at about 14,000 rpm, for example. No severe critical speed problems are apparent from this diagram. Measurements made of the critical frequencies are reported by Shreeve in Appendix B. Some discrepancies between Figure 2 and Figure B2 are noted, although the critical first bending mode was confirmed closely. The possibility of excitation of the unidentified modes by the 23 stator vanes should not be ignored.

The purpose of the honeycomb following the stators is to remove all of the tangential velocity from the flow leaving the compressor stage. The compressor inner casing is free to rotate about the axis but is restrained by a flexure for torque measurement (Fig. 5). The outer casing is also free to rotate to permit relative rotation of instruments with respect to the trailing edge of the stators. Rotation is restrained by the clamping arm and angular position indicated by the protractor segment shown on Figure 4.

4. DIFFUSER

The diffuser in this test vehicle serves both to recover some of the compressor exit kinetic energy and also to direct the exit flow radially outward, away from the drive turbine. An axisymmetric diffuser is used to minimize circumferential non-uniformities impressed on the flow leaving the compressor stage.

This curved diffuser is quite conservative in the area ratio that is used compared to straight annular diffusers investigated by Sovran and Klomp (Ref 4). The representative width-to-length ratio of this diffuser is $\Delta R/L = 4.26$, and the area ratio is 1.31. Maximum static recovery for a straight annular diffuser of this $\Delta R/L$ value would occur with an area ratio of about 1.75, with an expected increase in C_p from about 0.35 to about 0.7. Because of the 90° turn required, and non-uniform entry total pressure, conservatism was certainly advisable in the selection of this diffuser area ratio. Rakes have been installed to measure the exit total pressure profile. These results will indicate whether more recovery could be obtained.

5. INSTRUMENTATION

The axial compressor test rig is equipped with static pressure measuring orifices in the outer casing at about 20 axial stations from the inlet contraction to the stator exit, with the majority of the pressure taps concentrated in the region of the rotor and stator vanes (Fig 4). Locations for 12 high-frequency-response Kulite static pressure sensors are provided in the outer casing over the rotor blade tips and just upstream and downstream to permit determination of the blade-to-blade pressure field at the rotor tip. Probe survey stations are provided upstream of the rotor spinner, upstream and downstream of the rotor and downstream of the stator. The outer casing can rotate with respect to the stators so circumferential as well as radial surveying of the flow is possible. The probes used in each experimental investigation will be described in reports of those investigations. Fixed arrays of 20 Kiel total pressure probes and 13 shielded thermocouples have been used to measure stator outlet flow properties. The torque exerted on the stator vanes, the honeycomb and the inner casing (including the rotor windage) is measured by strain gages mounted on a flexure located between the rotor bearing housing and the inner casing (DWG 2147-1). Work input to the airflow can be measured by means of (1) torque, and rotor rpm; (2) temperature rise and airflow; and (3) change of tangential velocity, rotor rpm and airflow. Rotor speed can be measured to great accuracy under steady state conditions.

Airflow must be measured accurately because of the direct effect on all three methods of power input determination. For this reason considerable care was given to the flow measuring system described in section 3 entitled "Induction System".

6. CONCLUDING REMARKS

An interesting transonic axial compressor stage using a simplified design approach and using simplified rotor blade sections has been constructed. A useful comparison with more conventionally designed rotors, like GE design rotor 1B, should be available from tests of this NPS transonic compressor. Unfortunately, an error was made in calculating blade setting angles such that the tip section is about 5° too open. The suggestion is made that tests of similar shapes using the same alloy and same heat treatment to determine whether the rotor blades can accept a 5° -closed twist in the outboard region without danger of failure during subsequent testing. If so, the design intent can be tested.

Prediction of the flow conditions that should be expected from this rotor as built is not the subject of this design review; however, such analysis would be a useful study for comparison with the results of experiments using this rotor as built. This study might also help determine whether the stator built as part of the transonic axial compressor stage can be expected to function efficiently with this rotor.

TABLE I COMPRESSOR RIG DRIVE TURBINE DESIGN DATA

PRESSURE RATIO	= 2.8
STAG. TEMP.	= 640°R
FLOW RATE	= 10.85 lbs/sec
POWER	= 485 HP
SPEED	= 30,500 RPM
REFERRED HP	= 155,89 HP
" FLOW	= 4.31 lbs/sec
" SPEED	= 27,450 RPM

TABLE II TRANSONIC COMPRESSOR DESIGN DATA

PRESSURE RATIO	= 1.5+
FLOW RATE	= 15.7 lbs/sec
POWER	= 433 HP
SPEED	= 30,460 RPM
CASE DIAMETER	= 11 inches
HUB/TIP RATIO (Rotor Face)	= 0.5
TIP SPEED	= 1,462 ft/sec
BLADING:	
ROTOR	18 DCA BLADES (FLAT PRESSURE SIDE)
STATOR	23 DCA BLADES

TABLE III TRANSONIC COMPRESSOR AERODYNAMIC DATA

<u>ROTOR INLET (1)</u>	HUB	MEAN	TIP
R/R_O	.5	.791	1.0
U_1 (ft/sec)	731	1156	1462
λ_1 (deg)	31.75	10.5	0
V_1 (ft/sec)	801.7	693.3	681.7
β_1 (deg)	42.37	59.04	65.0
α_1 (deg)	0	0	0
<u>ROTOR EXIT (2)</u>			
R/R_O	.635	.825	1.0
U_2 (ft/sec)	928.4	2106.1	1462
λ_2 (deg)	16.5	6	0
V_{m_2} (ft/sec)	885.8	675.0	490.5
V_2 (ft/sec)	1005.8	784.6	663.2
V_{u_2} (ft/sec)	476.3	400.0	437.3
ΔT_t ($^{\circ}R$)	73.6	80.3	106.4
β_2 (deg)	27.03	50.07	64.42
$\Delta\beta_{\text{rotor}}$ (deg)	15.34	8.97	0.58
$\alpha_2 = \Delta\alpha_{\text{stator}}$ (deg)	28.27	30.65	42.30
<u>STATOR EXIT (3)</u>			
R/R_O	.668	.845	1.0
$V_3 = V_{a_3}$	676.8	712.0	591.0
<u>MACH NUMBERS</u>			
M_1 (absolute)	.757	.645	.634
Mw_1 (relative)	1.0246	1.254	1.500
M_2 (absolute)	0.909	0.683	0.557
Mw_2 (relative)	0.899	0.915	0.954
M_3 (absolute)	0.586	0.615	0.493

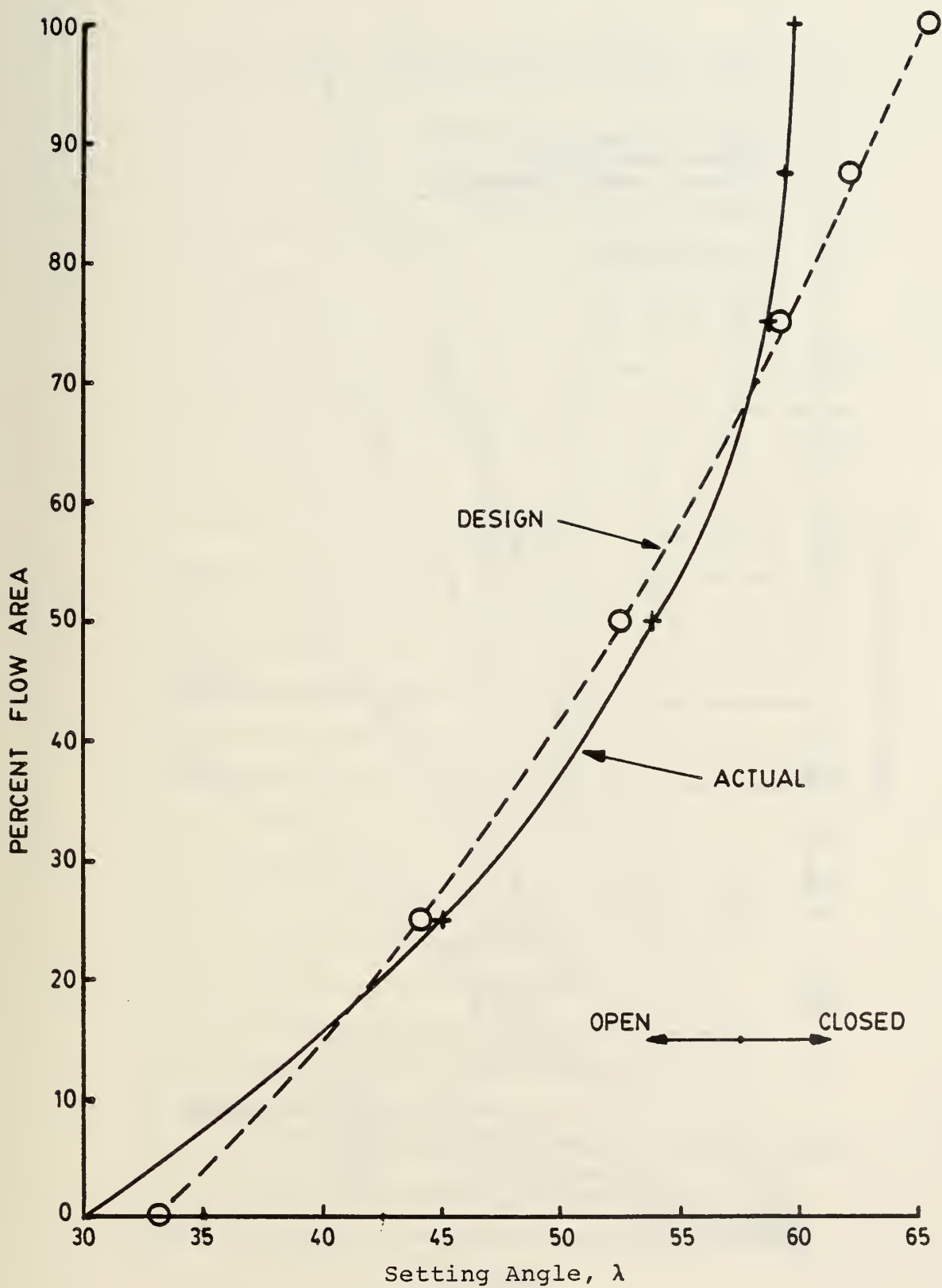


Fig 1. Rotor Blade Setting Angle

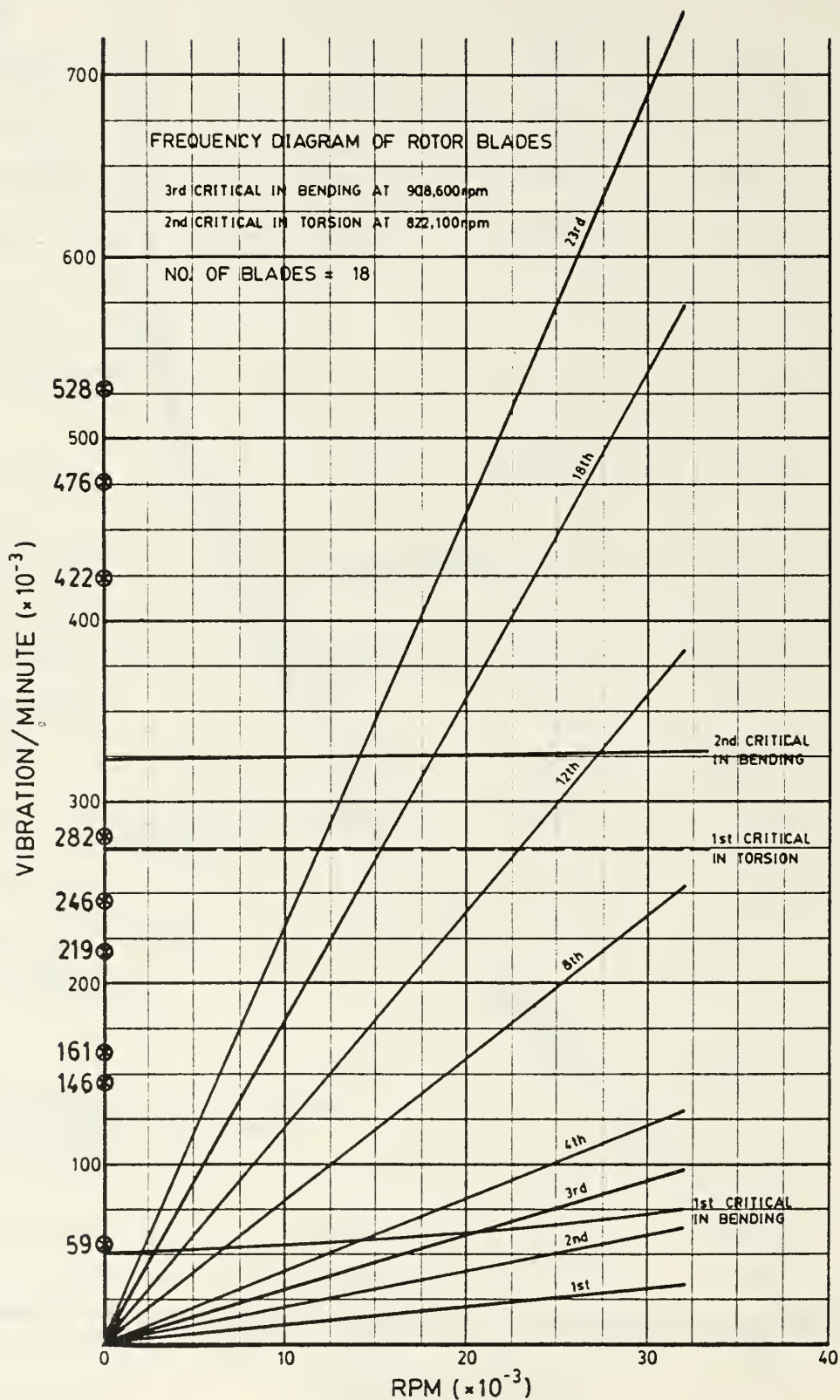


Figure 2. Design Campbell Diagram for the Transonic Rotor

(X) - Measured Critical Frequencies from Appendix B)

COMPRESSOR TEST RIG

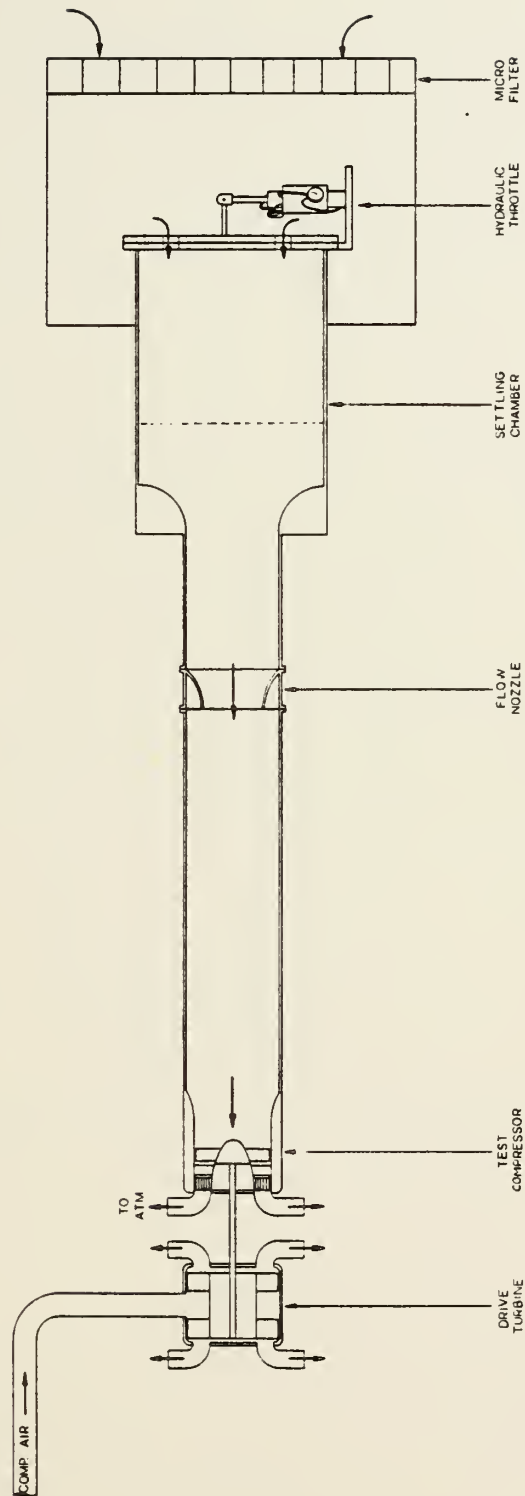
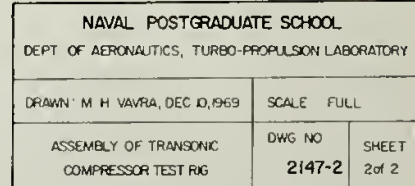


Figure 3. Transonic Compressor Test Rig
(not to scale)



APPENDIX A

EXPLORATORY STUDIES FOR THE DESIGN

Dr. M. H. Vavra studied possible transonic axial compressor airflow and pressure ratios combinations which could be driven by a cold air turbine using the air supply available in the Turbo-propulsion Laboratory of the NPS. His first considerations were for a small compressor (5" to 9" tip diameter) to produce a compression ratio of 1.75 with an assumed efficiency of 80%. These compressors would have required 138 to 445 horsepower to drive them. He sized radial turbines in the 300 to 400 hp range as potential power sources to drive the test compressor. Compressor tip speeds of from 1430 to 1480⁰ were contemplated. Apparently, the ease of obtaining shaft power from radial turbines led him to consider larger axial compressors, since the range of compressor outside diameters being examined was increased to 12 inches after the driving turbine design was considered. At this point, however, compressor shaft speeds were 2.73 times turbine shaft speeds so that a gear box was required.

Dr. Vavra at least briefly contemplated designing a centrifugal compressor rather than an axial transonic compressor. Comparisons of axial and centrifugal compressors of 12 inch outside diameters were made. The exit passage widths of the centrifugal compressors were found to be rather small (.5 to 1.2 inches) for accurate surveying and the absolute Mach numbers

rather high ($M = 1.07$ to 1.19). These considerations probably led Dr. Vavra back to concentrating on axial transonic compressors.

After selecting the type of compressor, Dr. Vavra devoted attention to a gear drive system capable of transmitting 500 hp with a turbine input rpm of 11,835 and a compressor drive speed of 32,200, a gear ratio of 2.72. A planetary system having 3 planet gears was selected. Gear tooth stress of 33,000 psi was calculated as compared to an endurance limit of 100,000 psi. Pitch line speed of 10,000 fps was selected. Bearing life was estimated to be 5,000 hours.

1. INTRODUCTION

The rotor of the transonic compressor was manufactured according to the drawings shown in Figure B1. Bench tests were carried out on the delivered rotor to establish critical frequencies for bending and torsional modes.

Two excitation techniques were used. First, the fundamental bending and torsional modes of each blade were indentified by bowing, using a powder to indicate nodal lines. Second, a shaker table was used to excite the complete assembly, and the higher order modes were observed from the outputs of strain gauges attached to one blade.

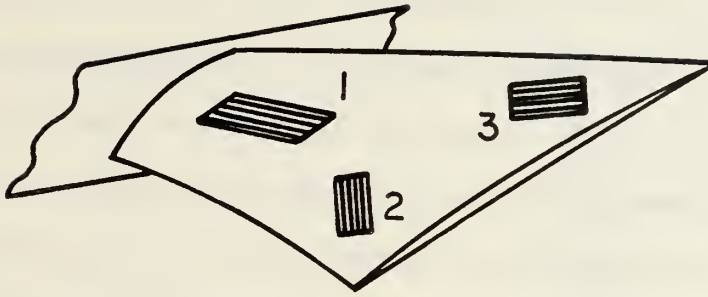
2. BOWING TESTS

The rotor was clamped in a vice and the rotor blades bowed in turn across the tip to excite the first bending modes. The pure tones produced were picked up by the microphone connected to the input of a Spectral Dynamics Model SD 330 Real-Time Analyzer.

The frequencies obtained for the lowest modes are shown for the eighteen blades of the rotor in Table B1. (The blade designated as Blade #1 was instrumented with strain gauges and was not bowed.)

3. SHAKER TABLE TESTS

Three strain gauges were attached to one rotor blade as shown in the following sketch:



The complete rotor was mounted on the table of a moving coil vibrator. The vibrator excitation frequency was varied from 0 to 10,000 cps while the amplified strain gauge outputs were selectively fed as inputs to the Spectral Dynamics Model SD 330 Real-Time Analyzer. The appearance of resonant peaks in the strain gauge outputs was recorded.

The data obtained is shown in Table B2. Note that the resonances at 1872 cps and 2680 cps were distinct and unambiguous.

4. DISCUSSION

Since the rotor blades and hub were machined as a single unit, the bowing technique was effective in exciting the bending critical frequencies. There was found to be a variation of $\pm 5.6\%$ in the frequencies of the bending modes excited in the different blades about an average value of 1005.5 cps. This is possibly evidence of variations in blade shape, particularly blade thickness, resulting from inaccuracies in the machining process. A variation of about $\pm .003$ inches in the blade thickness could explain the differences in first bending critical

frequencies. Because of blade twist, a simple measurement of blade thickness was not practical, and a more elaborate dimensional check of the delivered rotor was not attempted. However, the data obtained from a single blade in shaker table tests suggest that there might be more than one mode of oscillation involved in the data given in Table B1. Holographic observation of the blading, which would have indicated nodal patterns, was not available at the time of the tests.

The data from Table B2 is shown in a frequency speed diagram for the rotor in Figure B2.

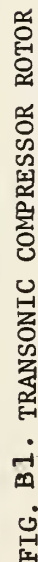
TABLE B1: FIRST BENDING MODE FREQUENCIES FOR TRANSONIC
COMPRESSOR ROTOR BLADES

<u>BLADES #</u>	<u>FREQUENCY (cps)</u>
1	--
2	1050
3	1040
4	1006
5	1020
6	1039
7	998
8	1004
9	1008
10	1012
11	999
12	946
13	974
14	936
15	998
16	996
17	1018
18	1050

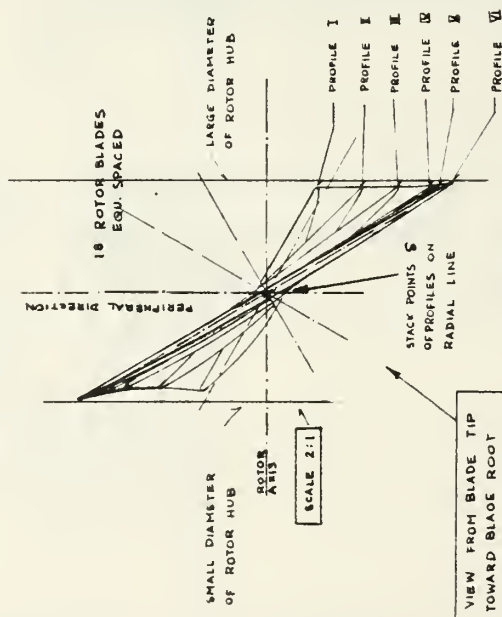
TABLE B2: SHAKER TABLE MEASUREMENTS OF VIBRATION MODES OF
TRANSONIC COMPRESSOR ROTOR BLADES

<u>FREQUENCY</u> (cps)	<u>STRAIN GAUGE OUTPUT (dbs)</u>		
	<u>#1</u>	<u>#2</u>	<u>#3</u>
8830	-37	-20	-23
7930	-27	-20	-16
7040	-40	-15	-22
4760	-36	-21	-32
4660	-41	-26	-35
4130	-32	-34	-31
4080	-34	-25	-28
3680	-39	-24	-27
3620	-30	-17	-21
2680	-21	-50	-32
2475	-25	-12	-18
2395	-31	-19	-21
1872	- 9	-45	-22
1180	- 9	-22	-36
1128	- 9	-24	-38
1046	-20	-35	-50
1026	-17	-34	-45
950	- 6	-22	-31

NOTE. Excitation amplitude = constant (0.21)
Wave analyzer input range = 0.316 v.RMS.
Wave analyzer output gain = 10 db. on log scale

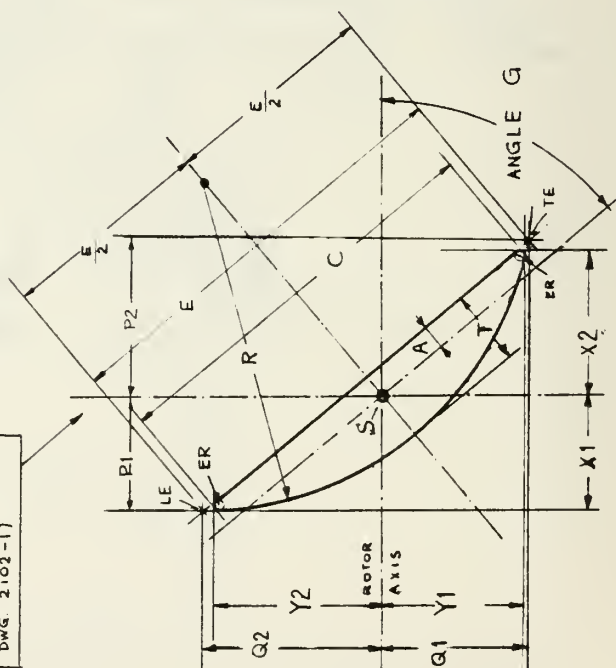


SYMBOL	PROFILE	I	II	III	IV	V	VI
D	DIAMETER OF CONE THRU STACKING RADIUS (SEE DWG. 2102-1)	4.242	7.669	8.886	9.968	10.480	11.000
H	ANGLE OF CONE THRU STACKING RADIUS (SEE DWG. 2102-1)	20° 42'	17° 52'	8° 32'	2° 28'	0° 47'	0
G	ANGLE BETWEEN PROFILE CHORD AND ROTOR AXIS	30° 05'	48° 03' 15"	53° 56' 40"	58° 48' 28"	59° 21' 42"	59° 49' 36"
C	PROFILE CHORD	1.463	1.792	2.100	2.389	2.537	2.688
R	RADIUS OF PROFILE CONTOUR	1.980	3.173	5.211	9.321	11.442	16.330
E	CHORD WITH SHARP LEADING & TRAILING EDGES	1.583	1.928	2.269	2.584	2.701	2.911
A	DISTANCE OF STACK POINT S FROM PROFILE CHORD	.067	.061	.050	.036	.032	.026
T	MAX. PROFILE THICKNESS	.165	.150	.125	.090	.080	.065
ER	LEADING AND TRAILING EDGE RADIUS	.015	.012	.010	.007	.005	.005
X1	DISTANCE OF PROFILE EDGE FROM S IN AXIAL DIRECTION	.609	.602	.589	.598	.625	.660
X2	DISTANCE OF PROFILE EDGE FROM S IN RADIAL DIRECTION	.661	.671	.655	.648	.671	.696
Y1	DISTANCE OF PROFILE EDGE FROM S IN PERIPHERAL DIRECTION	.329	.603	.827	1.007	1.078	1.152
Y2	DISTANCE OF PROFILE EDGE FROM S IN PERIPHERAL DIRECTION	.419	.672	.874	1.037	1.106	1.1732
P1	DISTANCE OF POINT LE FROM S IN AXIAL DIRECTION	.681	.638	.627	.639	.661	.709
P2	DISTANCE OF POINT TE FROM S IN AXIAL DIRECTION	.718	.724	.709	.701	.716	.754
Q1	DISTANCE OF POINT TE FROM S IN PERIPHERAL DIRECTION	.339	.640	.887	1.086	1.146	1.245
Q2	DISTANCE OF POINT LE FROM S IN PERIPHERAL DIRECTION	.455	.725	.947	1.124	1.178	1.271



- NOTES (1) BLADE SECTIONS SHOWN ARE TO BE WRAPPED ON CONES WITH THE DIAMETER "D" IN THE PLANE THRU THE RADIAL STACKING LINES. THESE CONES HAVE THE ANGLES "H" WITH THE ROTOR AXIS AS SHOWN IN DWG. 2102-1
- (2) THE BLADE PROFILES BETWEEN THE ONES SPECIFIED ON THE CONES ARE OBTAINED BY SMOOTH FAIRING.
- (3) THE ACTUAL HUB PROFILE IS OBTAINED BY THE INTERSECTION OF THE BLADE WITH THE SURFACE OF REVOLUTION OF THE HUB (3.85 RADIUS) SPECIFIED IN DWG. 2102-1
- (4) THE FILLET SHOWN IN DWG. 2102-1 MUST EXIST ALL AROUND THE HUB PROFILE AND ALSO FORWARD OF THE LEADING EDGE, AND DOWNSTREAM OF THE TRAILING EDGE, IN DIRECTION OF THE CHORD LINE.
- (5) TOLERANCES: FOR THICKNESS $\pm .001$
FOR CHORD $\pm .005$
FOR ANGLES ± 5 DEGREE

TYPICAL BLADE PROFILE (NO SCALE)
(PRESSURE SIDE IS STRAIGHT LINE)
(SUCTION SIDE IS A CIRCULAR ARC)
STACK POINTS S MUST LIE ON RADIAL STACKING LINE OF DWG. 2102-1



NAVAL POSTGRADUATE SCHOOL
DEPT. OF NAUTICAL ENGINEERING
NAVAL AVENUE
7/22/68
2102-1
2 OF 2
AS NOTED

TRANSOMIC COMPRESSOR TEST RIG
BLADING DATA OF TRANSOMIC ROTOR
2102-2

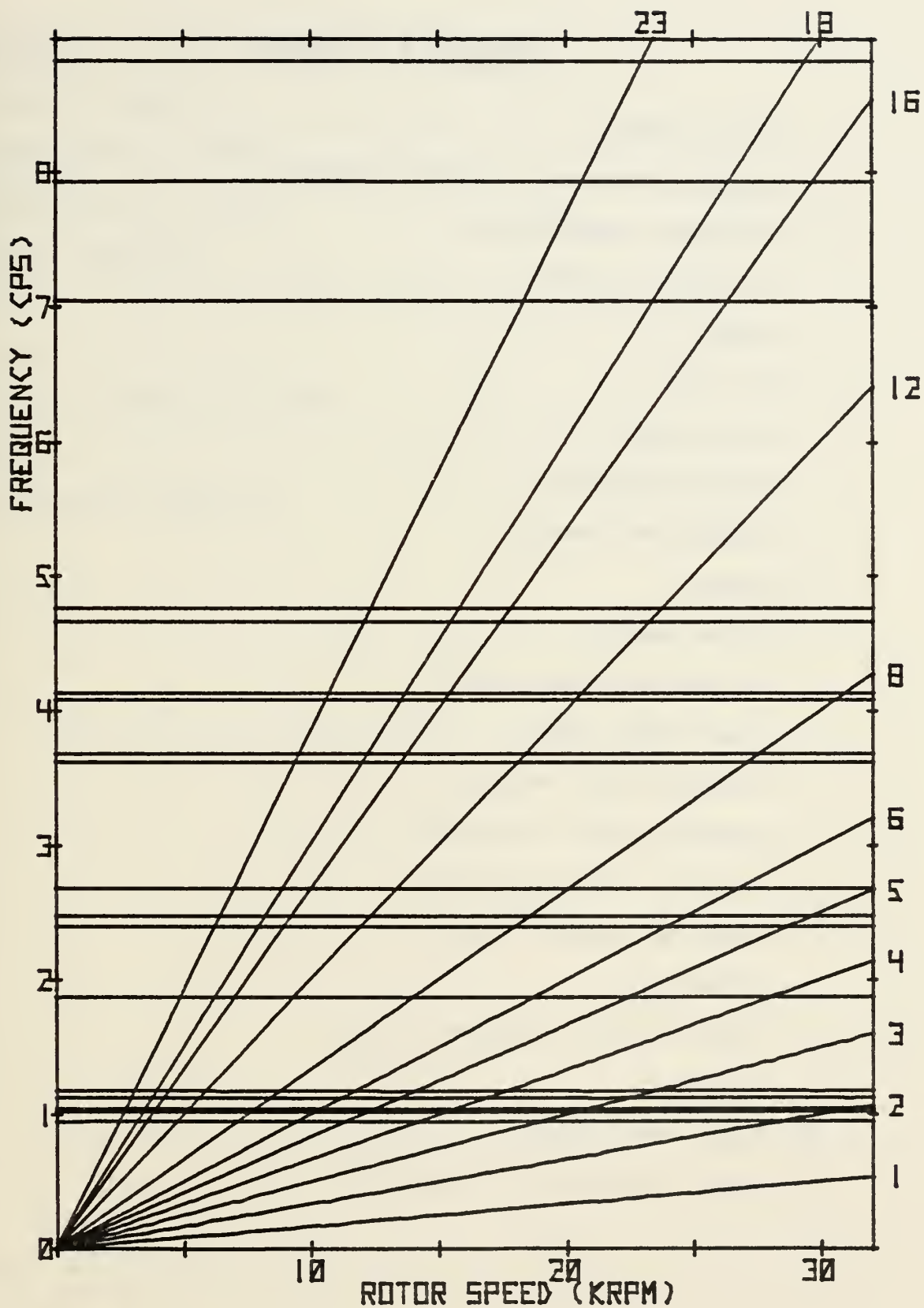


Fig.B2. FREQUENCY - SPEED DIAGRAM FOR BLADE VIBRATIONS FROM SHAKER-TABLE TESTS OF THE TRANSONIC COMPRESSOR ROTOR

APPENDIX C - SYMBOLS

c	- Chord length
C_p	- Specific heat at constant pressure
C_p	- Pressure coefficient
D	- Diffusion factor
L	- Length
\dot{m}	- Flow rate
M	- Mach number
p	- Static pressure
P	- Stagnation pressure
R	- Radius
s	- Blade spacing
T	- Stagnation Temperature
U	- Rotor blade speed
V	- Absolute flow velocity
α	- Absolute flow yaw angle
β	- Relative flow yaw angle
γ	- Ratio of specific heats
η	- Efficiency
λ	- Blade setting (stagger) angle
σ	- Solidity
$\bar{\omega}$	- Loss coefficient
Ω	- Total pressure loss parameter

Subscripts

- 1 - Ahead of rotor
- 2 - Downstream of rotor
- 3 - Downstream of stator
- a - Axial component
- H - Hub
- R - Rotor
- t - Total (stagnation) value
- T - Tip
- O - Peripheral component

References

1. Vavra, M. H. Aero-Thermodynamics and Flow in Turbo-machines,
2. NASA SP-36 Aerodynamic Design of Axial Flow Compressors, 1965.
3. Steinke, R. J. and Crouse, J. E., "Analytical Studies of Aspect Ratio and Curvature Variations for Axial-Flow-Compressor-Inlet Stage Under High Loading", NASA TN D-3959, 1967.
4. Sovran, G. and Klomp, E. D., "Experimentally Determined Optimum Geometrics for Rectilinear Diffusers with Rectangular, Conical or Annular Cross-Section", Fluid Mechanics of Internal Flow, edited by G. Sovran, Elsevier Publishing Co., New York 1967, pp 270-312.

DISTRIBUTION LIST

1. Commander
Naval Air Systems Command
Washington, DC 20361
Attention: Code AIR 310 1
Code AIR 310E 1
Code AIR 310F 1
Code AIR 320D 1
Code AIR 530 1
Code AIR 536 1
Code AIR 00D4 1
Code AIR 03D 1
2. Office of Naval Research 1
800 N. Quincy St.
Arlington, VA 22217
Attention: Dr. A. D. Wood
3. Commanding Officer 1
Naval Air Propulsion Center
Trenton, NJ 08628
Attention: V. Lubosky
4. Commanding Officer 1
Naval Air Development Center
Warminster, PA 19112
Attention: AVTD
5. Fan and Compressor Branch, MS5-9
NASA Lewis Research Center
21000 Brookpark Rd.
Cleveland, OHIO 44135
Attention: C. Ball 1
D. Sandercoch 1
N. Sanger 1
6. Library 2
Code 1424
Naval Postgraduate School
Monterey, CA 93943
7. Office of Research Administration(Code 0121) 1
Naval Postgraduate School
Monterey, CA 93943
8. Turbopropulsion Laboratory (Code 67Sf) 12
Naval Postgraduate School
Monterey, CA 93943

DUDLEY KNOX LIBRARY



3 2768 00347399 2